

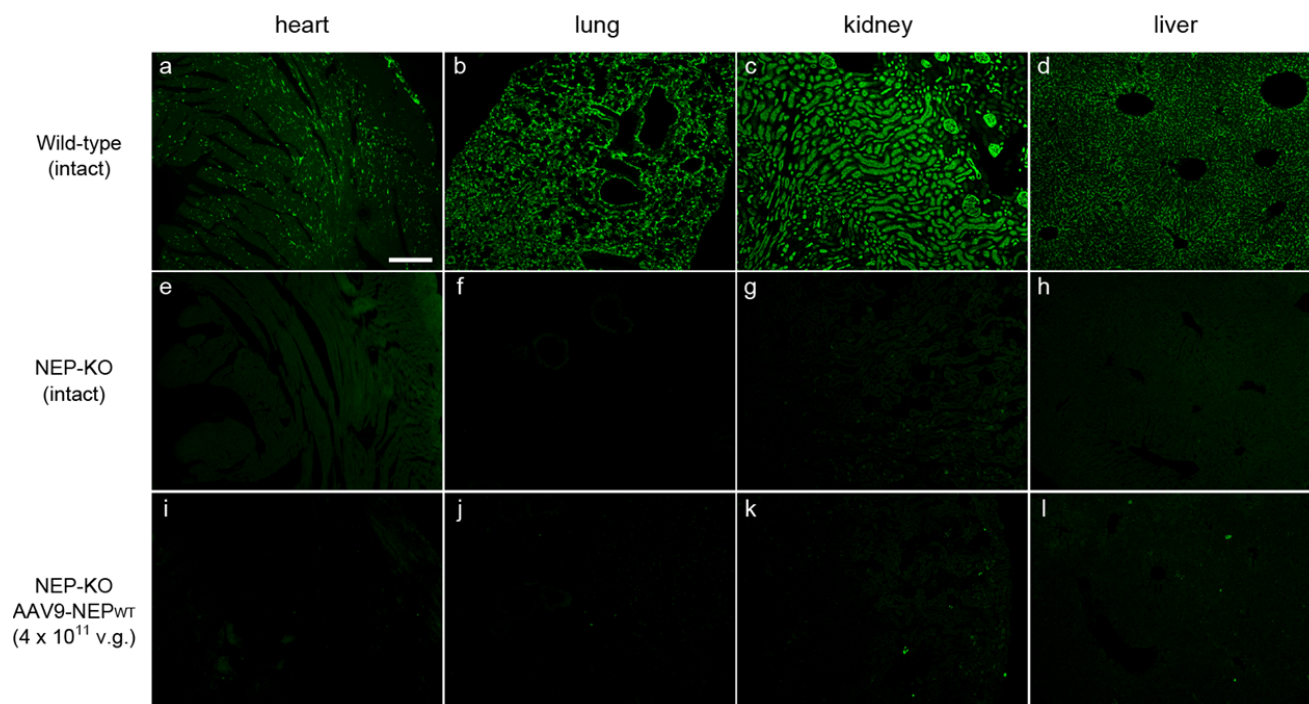
Supplementary information:

1. Supplementary Figure
2. Materials and Methods

Global brain delivery of neprilysin gene by intravascular administration of AAV vector in mice

Nobuhisa Iwata, Misaki Sekiguchi, Yoshino Hattori, Akane Takahashi, Masashi Asai, Bin Ji, Makoto Higuchi, Matthias Staufenbiel, Shin-ichi Muramatsu, and Takaomi C. Saido

Supplementary Figure 1



Supplementary Figure 1 NEP gene expression in peripheral tissues after intracardiac injection of the rAAV9.

NEP gene expression in several peripheral tissues, i.e., heart (**a,e,j**), lung (**b,f,j**), kidney (**c,g,k**) and liver (**d,h,l**), from neprilysin-knockout mice was investigated 14 days after intracardiac injection of rAAV9 with SynI promoter. The rAAV9 with Syn I promoter did not drive NEP gene expression in these tissues. Experimental conditions were the same as for Fig. 1. Scale bars, 20 μ m.

Materials and Methods

Antibodies.

Primary antibodies used in this study were as follows: anti-human neprilysin antibody (mouse monoclonal IgG₁, 56C6; 1:100 dilution; Novocastra, Newcastle, UK), antibody against either unmodified amino-terminus of A β , N1D (mouse monoclonal 82E1; 1:250; Immuno-Biological Laboratories [IBL], Gunma, Japan) or modified amino-terminus of A β , N3pE (mouse monoclonal 8E1; 1:250; IBL), anti-NeuN (rabbit polyclonal, 1:800; Millipore, Temecula, CA), anti-GFAP (guinea pig polyclonal; 1:200; Frontier Science, Hokkaido, Japan), FITC-conjugated anti-MAP2 (mouse monoclonal AP20; 1:50; Leinco Technologies, St. Louis, MO), anti-tau (mouse monoclonal IgG_{2a}, tau-1; 1:200 dilution; Millipore), anti-syntaxin-1 (rabbit polyclonal, 1:1,000; Merck, Darmstadt, Germany), anti-SV2A (rabbit polyclonal, 1:400; Synaptic Systems, Göttingen, Germany), anti-VAMP-1 (rabbit polyclonal, 1:1,000; Synaptic Systems), anti-PSD95 (rabbit polyclonal, 1:500; Synaptic Systems), anti-Rab3a (rabbit polyclonal, 1:1,000; Synaptic Systems), anti-Rab5 (rabbit monoclonal C8B1, 1:400; Cell Signaling Technology [CST], Danvers, MA), anti-Rab7 (rabbit monoclonal D95F2, 1:400; CST), anti-Rab9 (rabbit monoclonal D52G8, 1:400; CST), anti-clathrin heavy chain (rabbit monoclonal D3C6, 1:400; CST), anti-EEA1 (rabbit monoclonal C45B10, 1:400; CST), anti-syntaxin 6 (rabbit monoclonal C34B2, 1:400; CST).

AlexaFluor488-conjugated secondary anti-rabbit and anti-guinea pig antibodies and

AlexaFluor488-conjugated rabbit anti-FITC IgG for MAP2 were obtained from Invitrogen (San Diego, CA), FITC-conjugated goat anti-mouse IgG2a for tau1 was from SouthernBiotech (Birmingham, AL), TSA (Tyramide Signal Amplification) fluorescence and TSA biotin kits, Texas-Red-conjugated streptavidin for neprilysin staining were from Perkin Elmer (Waltham, MA), and EnVision plus system HRP-labeled polymer anti-rabbit antibody was from DAKO (Carpinteria, CA).

Behavioral Analysis.

Five months after the injection of rAAV vector into APP tg mice, the Morris water maze test was conducted as previously reported (1), with minor modifications. A circular maze made of white plastic (1 m diameter, 30 cm depth) was filled with water to about 20 cm in depth (22 to 23 °C). The water was colored with white paint so that mice could not see the platform (20 cm high, 10 cm diameter; 1 cm below the surface of water) or other cues under the water. There were some extra-maze landmark cues (i.e., calendar, figure, plastic box) that were visible to the mice in the maze. The movements of mice in the maze was recorded and analyzed with Image J WM (O'Hara, Tokyo, Japan). Mice received two trials (1 session) per day for four or five consecutive days. Each acquisition trial was initiated by placing an individual mouse quasi-randomly into the water facing the outer edge of the maze at one of four designated starting points, but the location of the submerged platform remained constant for each mouse throughout testing. A trial was terminated when the mouse reached the platform, and the time taken to

locate the escape platform (escape latency, sec), swimming distance (cm) and swimming velocity were determined in each trial. Cut-off time of the trial was 60s, and mice that did not reach the platform within 60s were removed from the water and placed on the platform for 30s before being towed off and placed back into their home cage. The inter-trial interval was about 4 hours.

***In vivo* imaging of amyloid and glial activation.**

Positron emission tomographic (PET) scans were conducted for APP tg mice at 20 months of age as described elsewhere (2,3) with a microPET Focus 220 animal scanner (Siemens Medical Solutions USA, Knoxville, TN) designed for small animals, which provides 95 transaxial slices 0.815 mm (center-to-center) apart, a 19.0-cm transaxial field of view (FOV) and a 7.6-cm axial FOV (35). Prior to the scans, the mice were anesthetized with 1.5% (v/v) isoflurane. Emission scans were performed for 60 min in a 3D list mode with an energy window of 350–750 keV, immediately after intravenous injection of an amyloid radiotracer [¹¹C]PIB (34.0 ± 3.0 MBq) or [¹¹C]Ac5216 (30.0 ± 3.5 MBq) for detecting upregulation of TSPO in activated glia. The two imaging sessions using different radiotracers were scheduled at least one day apart. All list-mode data were sorted into 3D sinograms, which were then Fourier-rebinned into 2D sinograms (frames, 10×1 , 8×5 and 1×10 min). Dynamic images were reconstructed with filtered back-projection using a 0.5-mm Hanning's filter. Volumes of interest were placed on multiple brain areas using PMOD[®] image analysis software (PMOD Group, Zurich,

Switzerland) with reference to an MRI template generated in a previous study (2). The radioligand binding in the hippocampus and neocortex was quantified by calculating the ratio of standardized uptake value (SUVR) in the target region to that in the reference region, and the cerebellum and striatum were used as references for [¹¹C]PIB and [¹¹C]Ac5216, respectively (3).

References

1. Huang, S.M., et al. *J. Biol. Chem.* **281**, 17941-17951 (2006).
2. Maeda, J., et al. *J. Neurosci.* **27**, 10957–10968 (2007).
3. Maeda, J., et al. *J. Neurosci.* **31**, 4720-4730 (2011).